



Optimized scaling of translational factors in oncology: from xenografts to RECIST

Downloaded from: <https://research.chalmers.se>, 2025-12-05 00:12 UTC

Citation for the original published paper (version of record):

Baaz, M., Cardilin, T., Lignet, F. et al (2022). Optimized scaling of translational factors in oncology: from xenografts to RECIST. *Cancer Chemotherapy and Pharmacology*, 90(3): 239-250.
<http://dx.doi.org/10.1007/s00280-022-04458-8>

N.B. When citing this work, cite the original published paper.



Optimized scaling of translational factors in oncology: from xenografts to RECIST

Marcus Baaz^{1,2} · Tim Cardilin¹ · Floriane Lignet³ · Mats Jirstrand¹

Received: 25 April 2022 / Accepted: 10 July 2022
© The Author(s) 2022

Abstract

Purpose Tumor growth inhibition (TGI) models are regularly used to quantify the PK–PD relationship between drug concentration and in vivo efficacy in oncology. These models are typically calibrated with data from xenograft mice and before being used for clinical predictions, translational methods have to be applied. Currently, such methods are commonly based on replacing model components or scaling of model parameters. However, difficulties remain in how to accurately account for inter-species differences. Therefore, more research must be done before xenograft data can fully be utilized to predict clinical response.

Method To contribute to this research, we have calibrated TGI models to xenograft data for three drug combinations using the nonlinear mixed effects framework. The models were translated by replacing mice exposure with human exposure and used to make predictions of clinical response. Furthermore, in search of a better way of translating these models, we estimated an optimal way of scaling model parameters given the available clinical data.

Results The predictions were compared with clinical data and we found that clinical efficacy was overestimated. The estimated optimal scaling factors were similar to a standard allometric scaling exponent of -0.25 .

Conclusions We believe that given more data, our methodology could contribute to increasing the translational capabilities of TGI models. More specifically, an appropriate translational method could be developed for drugs with the same mechanism of action, which would allow for all preclinical data to be leveraged for new drugs of the same class. This would ensure that fewer clinically inefficacious drugs are tested in clinical trials.

Keywords Translational research · Combination therapy · Oncology · Mathematical modeling · Nonlinear mixed effects

Introduction

A major problem in the drug development process in oncology is translating results from preclinical studies to a clinical setting [1, 2]. Clinical efficacy is frequently overpredicted, which means that test compounds showing promising preclinical results fail when they enter clinical trials [3, 4]. This is one of the main reasons for the high attrition rates seen

for anticancer drugs [5]. However, there exists a correlation between preclinical efficacy, estimated from studies using either patient-derived xenografts (PDXs) or traditional xenografts based on cell lines, and clinical efficacy [6–8]. This shows the potential of using xenograft mice for testing compounds, in particular PDXs as they represent the human disease condition better [9], but also highlights the need for further translational research.

Combination therapies have come to play a leading role in anticancer treatment during the last decades [10]. The strengths of this type of treatment are, *e.g.*, synergistic effects between the drugs and slower onset of resistance [11, 12]. However, giving two drugs concomitantly leads to complex pharmacokinetic (PK) as well as pharmacodynamic (PD) interactions that need to be analyzed [13]. Moreover, these effects can differ between species, making translational efforts even more challenging [14].

✉ Marcus Baaz
Marcus.Baaz@fcc.chalmers.se

¹ Fraunhofer-Chalmers Research Centre for Industrial Mathematics, Chalmers Science Park, 41288 Gothenburg, Sweden

² Department of Mathematical Sciences, Chalmers University of Technology, University of Gothenburg, Gothenburg, Sweden

³ Merck Healthcare KGaA, Darmstadt, Germany

Mathematical modeling is a powerful tool for drug development and, in particular, for evaluating combination therapies [15]. Typically, a tumor growth inhibition (TGI) model is developed and calibrated to xenograft tumor volume data [16–18], and then used to investigate the efficacy of alternative treatments scenarios such as different drug doses or treatment schedules [19]. However, inter-species differences have to be accounted for to make clinical predictions [20]. The translational methods that are currently used can primarily be divided into two categories: replacement of model components, *e.g.*, growth rate parameter, exposure, or even the entire PK model; and scaling of model parameters [21, 22]. However, these methods are often insufficient to accurately translate the relationship between drug dose or concentration and *in vivo* efficacy due to the physiological differences between tumor xenograft in mice and cancer progression in human [23]. A potential contributing factor is also inadequate experimental design [24]. Therefore, additional model-based translational approaches are needed to make full use of preclinical data and minimize drug attrition rates.

In this paper, we calibrate preclinical TGI models using xenograft data from the literature for three drug combinations. We then replace mice PK with human PK, accounting for differences in protein binding, and formulate a mathematical optimization problem to find how to best scale the PD rate parameters to describe published clinical data. We hypothesize that the optimal scaling factors could be drug/cancer type specific and could thus be used to leverage all preclinical data when developing new drug combinations for the same cancer type and with the same drug mechanisms of action. Finally, we compare the optimal scaling factor with the standard allometric scaling factor for rate parameters.

Methods

Data

Preclinical data

We analyzed PDX data for combination therapies for which we were also able to find clinical data in the literature. The PDXs had either cutaneous melanoma (CM) or colorectal cancer (CRC) and data for combinations of binimetinib/encorafenib (CM), binimetinib/ribociclib (CM), and cetuximab/encorafenib (CRC) were taken from Gao et al., 2015 [7]. Data for vehicle groups of the two cancer types and single agent data were also extracted. All-time series were cut at day 60 to better reflect a typical xenograft study. Exposure data for encorafenib and ribociclib in mice were extracted from the same publication, whereas data for the other two drugs were gathered from other sources [25, 26]. Treatment

schedules and sample size of each treatment group can be found in the Supplementary Information (Table S1).

Anticancer drugs can have different efficacy depending on the specific cancer cells mutations the patient has [27]. We have, therefore, stratified the data into BRAF-mutants, NRAS-mutants, and all other mutants. In the binimetinib/ribociclib combination group, there were five CM PDXs that had a mutation in the BRAF gene and five that had a mutation in the NRAS gene. There were 13 BRAF mutants and nine NRAS mutants in all other CM treatment groups. Among the CRC PDXs, there were only six BRAF mutants and a single NRAS mutant.

Clinical data

In clinical oncology studies, patient response is categorized using the RECIST criteria. The sum of the longest diameters for all target lesions (SLD) is measured at the start of treatment (baseline) and at subsequent checkups. Each patient is categorized based on their best response using four response categories: Complete Response (CR), Partial Response (PR), Progressive Disease (PD), and Stable Disease (SD) [28].

Clinical RECIST data were obtained from ClinicalTrials.gov. Data for the following treatment groups were available: binimetinib (NRAS/BRAF, CM) [29, 30], binimetinib/ribociclib (NRAS, CM) [31], encorafenib (BRAF, CM) [32], binimetinib/encorafenib (BRAF, CM) [32], cetuximab (CRC) [33], and encorafenib/cetuximab (CRC, BRAF) [34]. All drugs were given orally, except for cetuximab, which was given intravenously. Treatment schedule, sample size, checkup time, response rate, cancer type, and mutations for each clinical trial can be found in the Supplementary Information (Table S1). For more information regarding each study, the reader is referred to the corresponding article.

Preclinical modeling

Exposure to anticancer drugs

Daily unbound average concentration, $C_{avg,u}$, was used to describe the exposure to all drugs except binimetinib for which unbound maximum concentration, $C_{max,u}$ was instead used, as maximal concentration has been shown to correlate better with clinical efficacy than overall exposure for this particular compound [26]. The unbound concentrations were computed by first estimating the total average or maximum concentration, $C_{avg,tot}$ or $C_{max,tot}$, and then adjusting for *in vitro* mean unbound protein fraction in mice, $f_{u,Mouse}$ (17), according to

$$\begin{aligned} C_{avg,u} &= C_{avg,tot} \cdot f_{u,Mouse} \\ C_{max,u} &= C_{max,tot} \cdot f_{u,Mouse} \end{aligned} \quad (1)$$

$f_{u,Mouse}$ for each drug was extracted from the literature [25, 35–37]. Compartmental models were fitted to the extracted exposure data of encorafenib and ribociclib. One-compartment models were sufficient to describe the PK data of both compounds. For cetuximab, we used a one-compartment model from the literature [25]. These three models were used to estimate $C_{avg,tot}$ of encorafenib, ribociclib, and cetuximab in the TGI model. Due to lack of an adequate PK model for binimetinib, the $C_{max,tot}$ value was gathered from the literature [26]. Total and unbound exposure for each drug and treatment schedule are summarized in Table 1. A detailed description of how these values were derived is available in the Supplementary Information.

Tumor growth inhibition model

To quantify the preclinical anticancer efficacy of each drug and drug combination, a one-compartment TGI model was calibrated to each tumor type. The choice of this relatively simple model was made to balance model complexity with the amount of available data. In the model, all tumor cells are assumed to be proliferating and located in a single compartment. A schematic representation of the model is shown in Fig. 1.

Turnover of tumors cells exposed to drug i as single agent is described by the following differential equation,

$$\frac{dV}{dt} = (k_{ng} - a_i \cdot C_i) V(t), V(0) = V_0, \quad (2)$$

where V is the volume of tumor cells, V_0 the initial tumor volume, k_{ng} the net tumor growth rate constant, a_i the potency of drug i , and C_i average or maximum unbound drug concentration. T

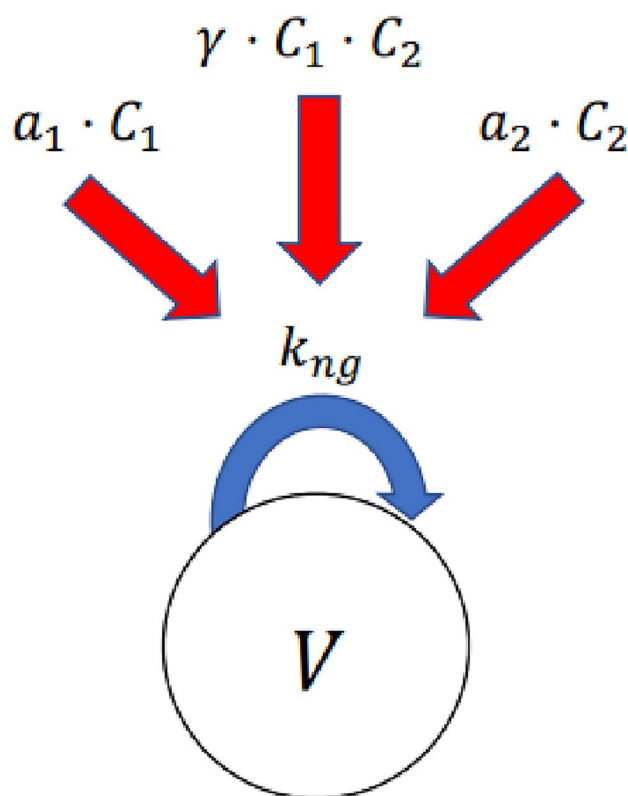


Fig. 1 A schematic representation of the TGI model for two drugs. V denotes the volume of the proliferating cells and k_{ng} the net tumor growth rate constant before start of treatment. C_i and a_i are the unbound concentration and potency of drug i , respectively. There is also a possible interaction term between the two drugs, denoted by γ_{ij} .

Table 1 Preclinical and clinical drug exposure

Drug	Dose schedule	Total exposure	f_u	Unbound exposure
Preclinical				
Cetuximab	20 mg/kg 2.q.w.	3235 µg/mL	1	3235 µg/mL
	20 mg/kg q.2.w.	893 µg/mL		893 µg/mL
Encorafenib	20 mg/kg b.i.d.	28 µg/mL	0.042	1.2 µg/mL
	20 mg/kg q.d.	14 µg/mL		0.6 µg/mL
Ribociclib	250 mg/kg q.d.	16 µg/mL	0.2	3.2 µg/mL
Binimetinib	10 mg/kg b.i.d.	1.2 µg/mL	0.015	0.02 µg/mL
Clinical				
Cetuximab [34, 38]	400/250 mg/m2 q.w.	3236 µg/mL	1	3236 µg/mL
Encorafenib [32]	300 mg q.d.	6.60 µg/mL	0.14	0.92 µg/mL
Encorafenib [32, 35]	450 mg q.d.	8.25 µg/mL	0.14	1.15 µg/mL
Ribociclib [31]	200 mg q.d.	4.00 µg/mL	0.3	1.2 µg/mL
Binimetinib[32]	45 mg b.i.d.	0.60 µg/mL	0.03	0.02 µg/mL

Specification of both total and unbound preclinical and clinical exposure for each drug and treatment schedule

When two drugs, i and j , are given in combination, the turnover is instead described by,

$$\frac{dV}{dt} = (k_{ng} - a_i \cdot C_i - a_j \cdot C_j - \gamma_{ij} C_i C_j) V(t), \quad (3)$$

where γ_{ij} is included to describe a potential synergistic or antagonistic effect between the drugs [9].

Mathematical modeling and parameter estimation were performed using an NLME framework (more details are found in Computational Methods). One TGI model for each cancer type was fitted to the data and log-normal between-subject variability (BSV) was accounted for on the parameters k_{ng} and V_0 in both models and on the potency parameter of binimetinib, a_{Bini} , in the CM model. No correlation between random effects was assumed and a proportional observation error was used in the model based on residual analysis. We also investigated if there was a significant difference between parameter estimates if treatment groups were stratified in BRAF-mutants, NRAS-mutants, and others.

Clinical modeling

Translational

To predict clinical response, translational methods were applied to the preclinical TGI models. Initially, we only replaced mouse exposure with human exposure, after accounting for differences in protein binding [20, 21]. For each drug, reported AUC_{tot} or $C_{max,tot}$ values were taken from the clinical study if available, or otherwise values from similar studies. The exposure was then adjusted by in vitro mean unbound protein fraction in humans, $f_{u,Human}$ [6, 24, 35, 36]. Total and unbound exposures for each drug and treatment schedule are summarized in Table 1. A detailed description of how values were derived is available in the Supplementary Information.

Clinical predictions

We used our translated preclinical TGI models to predict the proportion of patients in each RECIST category. To do this, two important aspects first had to be considered. First, the RECIST criteria are based on SLD, whereas predictions from the models are on volumes. Therefore, we converted the volume predictions to SLD by assuming either spherical or ellipsoid tumors [39]. In the ellipsoid case, prolate ellipsoids were assumed as well as that tumor growth or shrinkage only occurs along the longest radius. This leads to the volumetric change being the same as the change in SLD between two time points. For the spherical case, the volumetric change has to be greater than the SLD change

to achieve CR/PR or PD [28, 39, 40]. Both assumptions of spherical and ellipsoid tumors were evaluated in this paper.

Second, only the best response, which can occur at any checkup, for each patient is reported in the clinical studies. Therefore, we made the simplifying assumption that the best response occurred at the first evaluation, *i.e.*, at week 6 or 8, and we called this time T . We subsequently investigated how the predictions were affected if a different T was chosen.

To make the predictions, we used the translated preclinical model (formed by the preclinical tumor model combined with the human PK) to generate 1000 studies with the same number of individuals as in the original study. The time evolution of tumor volume of each individual was simulated and converted to SLD. After that, the percentage change between baseline and week T was calculated, using the following equation,

$$\Delta SLD = 100 \cdot \frac{SLD_T - SLD_0}{SLD_0}. \quad (5)$$

A patient is classified as CR&PR if $\Delta SLD \leq -30$, as PD if $\Delta SLD \geq 20$, and as SD if $-30 \leq \Delta SLD \leq 20$ [28]. This process of generating and categorizing individuals is illustrated in Fig. 2.

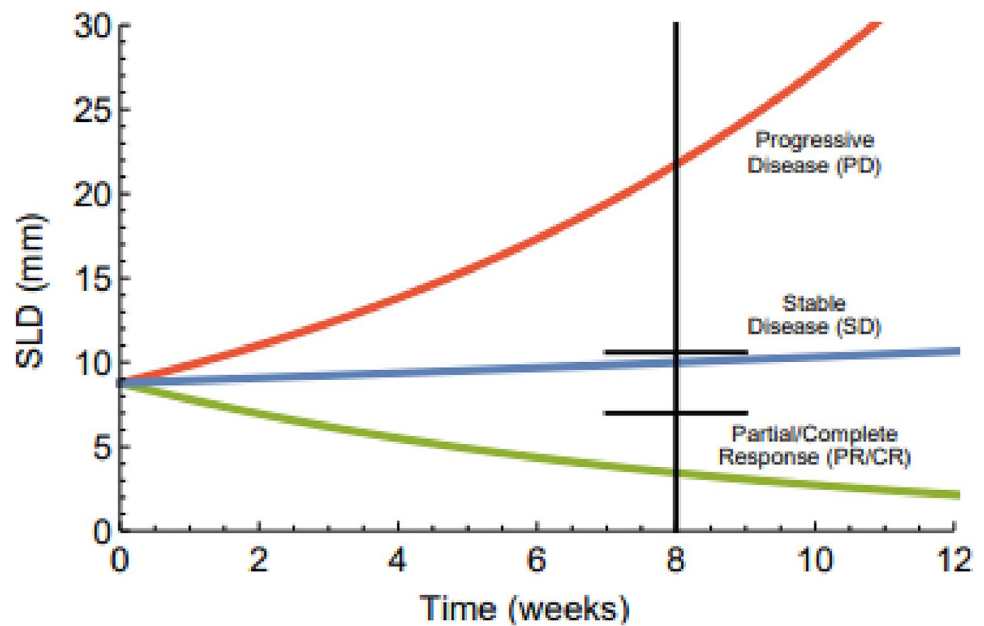
Each individual's ΔSLD was compared with the RECIST thresholds and thus, the proportion of patients in each RECIST category was estimated for each study. Subsequently, mean and 95% confidence interval (PCI) of each RECIST category was calculated. We considered a prediction to be adequately good if the PCI covers the clinical data observation.

Optimization

After making our predictions with the translated models we wanted to investigate how the parameters in the model should be scaled to describe the clinical data better. The parameters that we focused on were the PD rate parameters, k_{ng} , a_i , and γ_{ij} . We allowed the scaling of these parameters to be different and denoted the optimal scaling factors for them by A, B, and C, respectively. The optimal scaling factors were introduced to the model using the following expressions and were found by formulating and solving an optimization problem.

$$\begin{aligned} k_{ng}^H &= A \cdot k_{ng}^M \\ a_i^H &= B \cdot a_i^M \\ \gamma^H &= C \cdot \gamma^M \end{aligned} \quad (6)$$

Fig. 2 An illustration of how clinical predictions are performed. The color of green, blue, and red denotes classification into PR/CR, SD, or PD, respectively. The change in SLD between baseline and week 8 (black, vertical line) is compared to classify each individual



Here the superscript, M , denotes that the parameter is estimated from PDX data and, H , that the parameter is scaled for human predictions.

To formulate the optimization problem, we denoted the clinically observed and predicted percentage of patients in RECIST category i for treatment group j by y_{ij} and y_{ij}^* , respectively. Furthermore, y_{ij}^* is a function of the scaling factors $x = (A, B, C)$. A least-squares problem was formulated to find x such that the difference between y_{ji} and y_{ij}^* is minimized for all i and j . Mathematically this is described by the equation,

$$f(x) = \sum_{i,j} \left(y_{ij}^*(x) - y_{ij} \right)^2. \quad (7)$$

However, this objective function can lead to optimal solutions where some RECIST categories are not adequately predicted, which is compensated by very accurate predictions of other categories. Thus, to improve the predictions, on a study level, we penalized the solution for each RECIST category in y that was not covered by the PCI. This promotes solutions with as many adequate predictions as possible and was done by introducing the following penalty term,

$$\lambda \sum_{i,j} g_{ij}(x) = 0, \quad (8)$$

where λ is a penalty constant and,

$$g_{ij}(x) = \begin{cases} 0 & \text{if } y_{ij} \in PCI_j \\ 1 & \text{if } y_{ij} \notin PCI_j. \end{cases} \quad (9)$$

Combining this penalty term with Eq. 7 results in the following equation,

$$L(x) = f(x) + \lambda \sum_{i,j} g_{ij}(x). \quad (10)$$

The optimization problem was formulated as,

$$\text{minimize } L(x), \text{ subject to } -\infty < x \leq 0. \quad (11)$$

The optimization procedure was validated by first synthesizing data with known optimal scaling factors and then re-estimating these known factors. To give an idea of the uncertainty of the estimates, a non-parametric bootstrap was performed to calculate RSE % of each optimal scaling factor.

Allometric scaling

The heart rate of organisms has been shown to be proportional to the body weight of the organism raised to power of -0.25 [41]. This is the underlying rationale for some to propose that parameters associated with tumor growth can also be allometric scaling with exponent -0.25 [42]. Standard values of the body weight of a human and a mouse are assumed to be 70 kg and 20 g, respectively, which results in a scaling factor of approximately 0.13. We compared this scaling factor with the optimal scaling factors we found through our optimization procedure.

Computational methods

Mathematical modeling and parameter estimation were performed using an NLME modeling approach based on

the first-order conditional estimation (FOCE) method. The computational framework used was developed at the Fraunhofer-Chalmers Research Centre for Industrial Mathematics (Gothenburg, Sweden) [43]. The preclinical TGI models were simultaneously fitted to tumor volume data from all treatment groups of the same cancer type. The models were introduced based on the precision of estimated parameters, individual fits, empirical Bayes estimates (EBEs), Akaike information criterion (AIC), and visual predictive checks (VPC). We used Simulated Annealing and set λ to 1000 to solve the optimization problem. Mathematica was used to create all figures and to perform all computations.

Results

Preclinical modeling

Pharmacodynamics

The preclinical TGI models were able to describe the xenograft data adequately. Two outliers were removed from the

cetuximab (CRC) and encorafenib (CM) treatments groups. Examples of individual fits and parameter estimates are shown in Fig. 3 and Table 2, respectively. Fits to the entire dataset can be found in the supplementary information (Figs. S4–S13). VPCs can be found in the Supplementary Information (Figs. S1 and S2). All model parameters were estimated with acceptable precision.

Mutations did not significantly affect the net tumor growth rate constant or initial tumor volume. However, a significant difference in potency of encorafenib and binimetinib was found between different mutations. BRAF mutated PDXs responded considerably better to encorafenib than other PDXs. The potency parameter of encorafenib for BRAF-mutated CM PDXs was estimated to be $0.12 \text{ mL}/(\mu\text{g} \cdot \text{day})$, whereas no effect could be estimated for non BRAF-mutated CM PDXs. Since there were only six BRAF mutated CRC PDXs among 43, no significant encorafenib potency could be estimated for this sub-group either. Only the model describing the combination of cetuximab with encorafenib required an interaction term, which was estimated with good precision to $2.6 \cdot 10^{-5} \text{ mL}^2/(\mu\text{g}^2 \cdot \text{day})$.

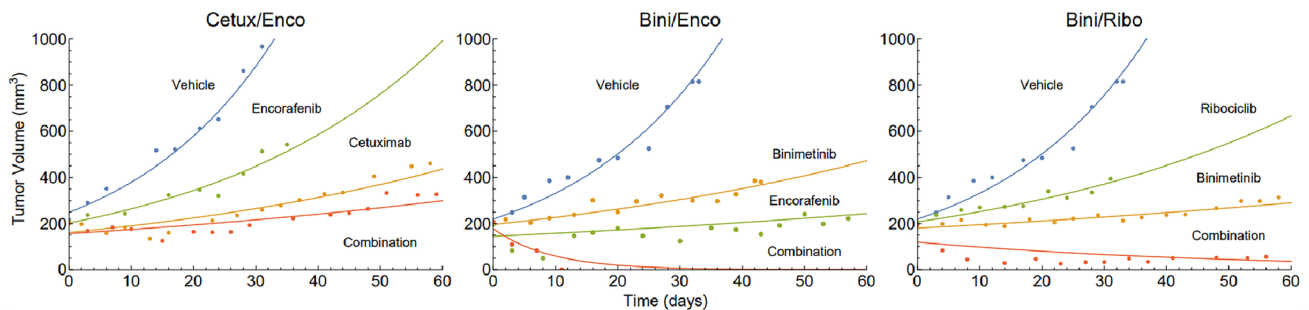


Fig. 3 Tumor volume versus time for one individual per treatment group and drug combination. Continuous lines are model predictions and dots experimental observations

Table 2 Parameter estimates

	Parameter	Unit	Estimate (RSE %)	BSV (RSE %)
Colorectal cancer	k_{ng}	1/day	0.05 (6)	71 (12)
	V_o	mm^3	235 (2)	24 (12)
	a_{Cetu}	$\text{mL}/(\mu\text{g} \cdot \text{day})$	$9.4 \cdot 10^{-6}$ (9)	
	a_{Enco}	$\text{mL}/(\mu\text{g} \cdot \text{day})$	0 (-)	
	$\gamma_{Cetu,Enco}$	$\text{mL}^2/(\mu\text{g}^2 \cdot \text{day})$	$2.6 \cdot 10^{-5}$ (9)	
Cutaneous melanoma	k_{ng}	1/day	0.06 (6)	53 (15)
	V_o	mm^3	200 (2)	22 (14)
	a_{Enco}	$\text{mL}/(\mu\text{g} \cdot \text{day})$	0.12 (10)	
	a_{Ribo}	$\text{mL}/(\mu\text{g} \cdot \text{day})$	0.013 (9)	
	a_{Bini}	$\text{mL}/(\mu\text{g} \cdot \text{day})$	1.7 (19)	61 (35)

Estimated PD parameters after fitting the two TGI models to the xenograft tumor volume data
RSE relative standard error

Clinical modeling

Clinical predictions

The preclinical TGI models were translated and clinical predictions were made for each treatment group where clinical data was available. As the predictions using ellipsoid tumors were in better agreement with the clinical data for the time-frame we used, we only present these predictions. A plot showing how the predictions are affected by the choice of T can be found in the Supplementary Information (Figure S3). The predictions, including predictions using allometric scaling, plotted against the clinical data for each treatment group are shown in Fig. 4, and in Table S4 in the Supplementary Information.

Optimization

The result of the validation procedure of the optimization method is found in the Supplementary Information (Table S2). The optimization problem, formulated in, Eq. 11, was solved separately for four monotherapy treatment groups. The optimal scaling factors (A, B) for each drug, along with RSE of each estimate and clinical predictions, can be found in the Supplementary Information (Table S3).

The optimization problem was also solved for the drug combinations. The preclinical cetuximab/encorafenib TGI model was the only combination with an interaction term and, therefore, three scaling factors. Results from the optimization for each drug combination are shown in Table 3. How well the translated models, using these optimal scaling factors, were able to describe the clinical data are shown in the last row of Fig. 4 and in the Supplementary Information (Table S4).

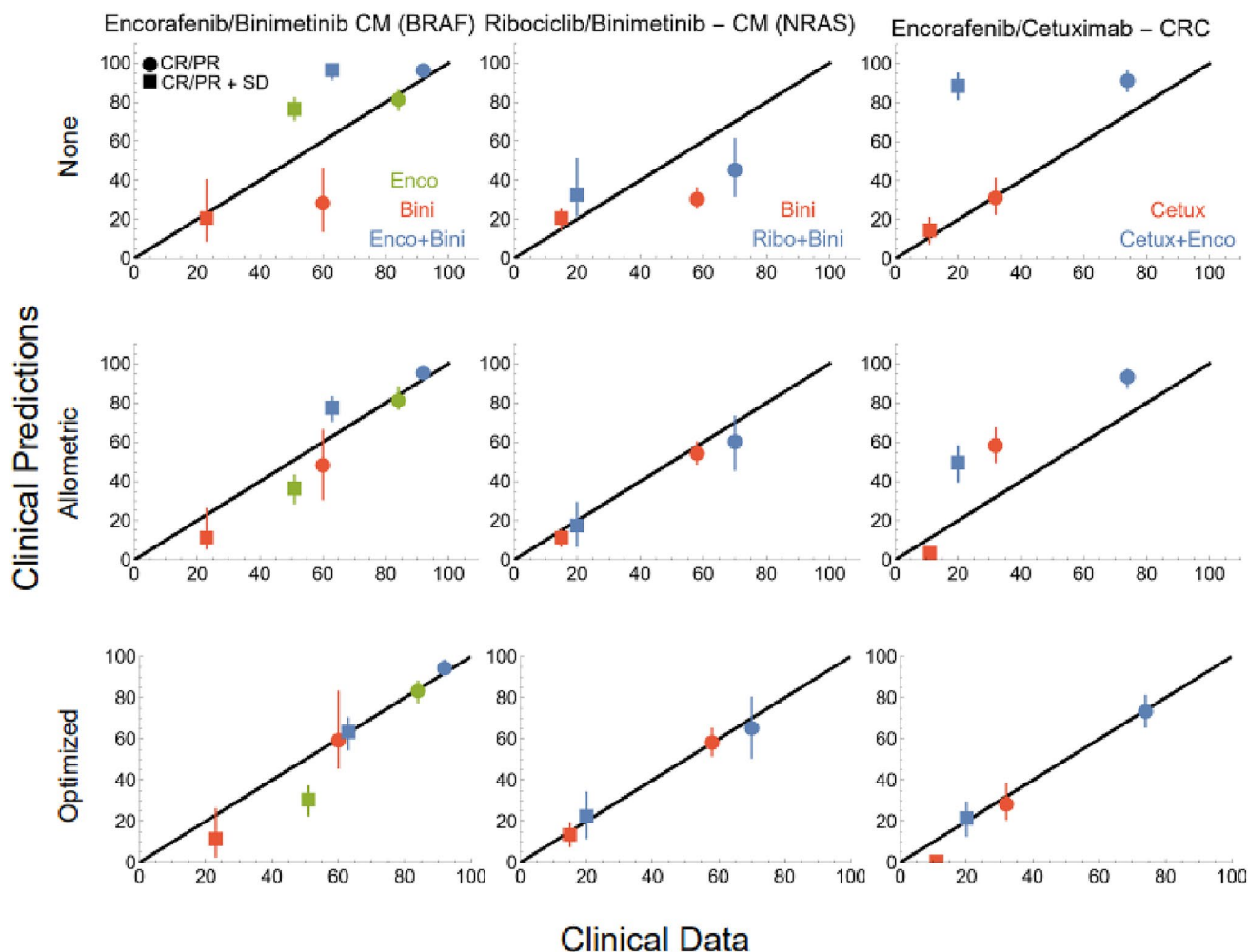


Fig. 4 (Row 1 and 2) Clinical predictions plotted against clinical data for all drug combinations and using both replacement of PK and allometric scaling. (Row 3) Illustration of how well the translated model,

using the optimal scaling factors could describe the clinical data. Color denotes treatment group and circles represent the response categories CR/PR and squares CR/PR + SD

Table 3 Optimization results

Treatment (cancer)	A (RSE %)	B (RSE %)	C (RSE %)
Monotherapies			
Enco (CM-BRAF)	0.20 (9)	0.20 (6)	–
Bini (CM-BRAF)	0.17 (3)	0.23 (3)	–
Bini (CM-NRAS)	0.14 (5)	0.18 (7)	–
Cetux (CRC)	0.85 (16)	0.78 (16)	–
Combinations			
Bini/Enco	0.07 (19)	0.09 (17)	–
Bini/Ribo	0.12 (10)	0.14 (11)	–
Cetux/Enco	0.21 (15)	0.09 (45)	0.13 (10)

Optimal scaling factors, with RSE, for each drug and drug combination

Discussion

Preclinical modeling

Exposure

The use of unbound concentrations is vital to account for differences in protein binding of species. This is especially the case for highly bound drugs, as a slight difference in protein binding can significantly affect the active drug concentration at the target site [44]. However, a limitation of using unbound fractions, estimated in vitro, is that it can be misleading as it does not necessarily describe the free concentration at the target site accurately [45]. Despite this, we do still believe that the approach we have used is the most appropriate for the data available to us.

In the final preclinical PD model we used a single value ($C_{avg,u}$ or $C_{max,u}$) to represent the exposure of the different drugs. These were chosen based on information from the literature what correlated best with clinical efficacy. We also tested using the simulated PK profiles of both encorafenib and binimetinib to drive the PD model, but this did not alter the fit.

Since clinical tumor measurements are typically performed quite infrequently (*e.g.*, once every 8th week) we do not believe that a more dynamical PK model than the one we used would significantly improve the model predictions.

Pharmacodynamics

Pharmacodynamic model

The PK-PD relationship between drug concentration and in vivo efficacy is commonly described by linear expressions, with the possible inclusion of an interaction term [46, 47]. Since the drugs we investigated were only tested at one dose level, the preclinical TGI models used need to match

this lack of richness in the experimental data. The choice of a relatively simple model was made after testing other models as well, *e.g.*, the Simeoni model (13), but not being able to estimate all parameters with sufficient precision given the available data.

All treatment groups with PDXs created from the same cancer type were fitted simultaneously and the models were able to describe the xenograft tumor volume data adequately. All model parameters were estimated with acceptable precision. The models were able to describe the data on both an individual level as well as on a population level, as can, *e.g.*, be seen in the individual fits and VPCs, respectively.

Analysis of mutations

Our predictions of the potency of each drug with regards to mutation are in agreement with the result from previous studies. BRAF-inhibitors, to which encorafenib belongs, are efficacious against BRAF-mutated CM but not against NRAS-mutated CM, which is what the model also predicted [48]. Moreover, the CRC PDXs seemed to be insensitive to encorafenib, given as monotherapy, however, the analysis is biased by the limited number of CRC BRAF-mutants in the dataset used.

Clinical predictions

Predictions versus data

Clinical predictions were made for all three drug combinations using the translated preclinical TGI models. With mice PK replaced with human PK, the model tended to overpredict the drug efficacy. This overprediction can, to some extent, be explained by the fact that the drugs were only tested on one preclinical dose level and, therefore, the model potency functions had to be extrapolated. Moreover, encorafenib was found to only have an effect when it was given as a combination to CRC PDXs, and thus the need to extrapolate the interaction term further explains the overprediction of the cetuximab and encorafenib combination. Having preclinical data for multiple dose levels would have been optimal, to minimize prediction errors coming from extrapolation.

Another aspect that must be considered is BSV and inter-study variability (ISV). BSV was included in on the tumor growth rate parameter to account for significant variability observed in the preclinical vehicle group. However, as there are no vehicle group in clinical studies it could be hard to quantify how much of the clinical variability comes from differences in tumor growth and drug sensitivity. ISV can be quite large when studies are conducted at different time periods, locations, or by different scientists [38]. As the data we

have used have been taken from different literature sources, we expected significant inter-study variability.

Furthermore, the predictions are also affected by the choice of model. We used semi-mechanistic models, and it would be interesting to investigate how much the predictions could be improved if more mechanistic models instead were used. To better mimic the human disease condition tumor regrowth or the appearance of new lesions could for example be included in the model. However, the model complexity is limited by shortcomings of PDXs such as they *e.g.*, only have one tumor lesion.

To evaluate what type of model is more suitable for this type of translational research, the cost, in terms of model complexity and biological knowledge, could be compared with the improvement in predictions. To perform such an evaluation, richer datasets, including different dose levels both in monotherapy and in combination may also be needed.

Assumptions

We made two assumptions in our clinical prediction: how to convert volumetric model predictions to diameters and when the best response of the patients occurred. Evidence has previously been put forward that assuming an ellipsoid tumor geometry is a better prognostic indicator of overall survival than a spherical one [39, 40]. Overall survival is thought to be correlated to response rates [49] and thus, it follows that ellipsoids should be more suitable for classifying patient response. Our findings further showed the superiority of assuming ellipsoid tumors, as these predictions were in better agreement with the clinical data.

Furthermore, we assumed that the best response of all patients occurred at the first checkup, *i.e.*, after 6 or 8 weeks from the start of treatment. We based this assumption on two studies that found that change in tumor volume at week 8 [50] and after two cycles of chemotherapy [51] correlated significantly with overall survival. We also analyzed how this assumption affects the predictions by varying the time of best response, which we call T . The number of patients that are classified as SD will shrink towards zero as T is increased. Moreover, the predictions from our approach will converge towards those using the Tumor-Static Concentration concept [52], as T becomes sufficiently large (see Figure S3 in the Supplementary Information). Figure S3 could be used to investigate what the best choice of T is. However, in our approach we chose to fix T and instead focus the investigation on how the predictions were affected by scaling the model parameters.

Other researchers who also have predicted clinical response rates from PDX data have made similar time frame assumptions. For example, Wong et al. [6] compared pre-clinical TGI after three weeks with clinical response rates

and Lindauer et al. [22] simulated tumor volumes and categorized the population at 0, 1, 3, and 6 months after treatment started. Pierrillas et al. proposed a different approach for comparing preclinical and clinical efficacy based on allometric scaling of the time frame [53]. They compared preclinical model predictions with human PD responses after 42 days of treatment, which compares well with our assumption of 6–8 weeks.

Optimal scaling factors

Optimization problem

The optimization problem was first solved for single agents and then for all three drug combinations. RSE of the optimal scaling factors was also calculated through a bootstrap procedure. The results from single agent optimization showed that the optimal scaling factors were all estimated with acceptable precision and were greater than the allometric scaling factor.

The optimal scaling factors for the cetuximab/encorafenib combination ranged from 0.09 to 0.21, which is significantly larger than the range of the factors of the other two combinations. However, as it was the only combination that showed a significant interaction effect, this difference in range is somewhat hard to interpret. It could indicate the need for different scaling approaches than the one we used when modeling combination therapies with significant potency interaction effects.

Comparison with allometric scaling

The allometric scaling relationship applies to endogenous mouse and human tumors, and some consideration has to be made to PDXs. In PDXs, human tumors are growing in mouse microenvironments and, therefore, there may exist a scaling factors that better captures the differences between PDXs and humans.

The optimal scaling factors that we found were quite close to the standard allometric scaling factor, giving some validity to the idea of scaling TGI models in this way. However, as can be seen in Fig. 4, standard allometric scaling was not sufficient to predict clinical response for all the combinations under study. Thus, showing that in order for the predictions from the translated preclinical TGI models to fit the clinical data for the combination therapies under study, the PD rate parameters had to, in general, be scaled down more than the allometric theory suggests. This demonstrates the need for new and improved scaling techniques, which might be found by testing our optimized scaling method on a more extensive dataset. A more suitable scaling factor, possibly specific to

cancer type and mechanism of action of the drug(s), could then be proposed. This factor would be used to describe the differences between humans and xenograft mice more accurately and would allow all preclinical data to be leveraged early in the drug development process. This should help in reducing the risks of bringing clinically inefficient drugs to the clinical development stage.

Conclusions

The predicted clinical efficacy of the three drug combinations was generally overestimated from the translated preclinical TGI models. More informative preclinical data in combination with a more complex model could potentially improve the predictions.

We developed a methodology for finding an appropriate scaling factor for TGI models. The methodology was applied to the drug combinations and we found that the optimal scaling factors were generally smaller than what allometric scaling suggests. However, more drug combinations have to be analyzed before a general factor can be proposed. To continue exploring and improving the translation capability of semi-mechanistic model, more data is required.

Supplementary Information The online version contains supplementary material available at <https://doi.org/10.1007/s00280-022-04458-8>.

Author contributions MB performed the research. MB and TC analyzed the data. MB, TC, FL, and MJ wrote the manuscript and designed the research.

Funding Open access funding provided by Chalmers University of Technology. Marcus Baaz was supported by an educational research grant from Merck KGaA, Darmstadt, Germany (CrossRef Funder ID: 09945).

Data and code availability The preclinical data can freely be accessed from Gao et al. [1]. All supporting Mathematica code is available from the corresponding author on reasonable request.

Declarations

Conflict of interest Floriane Lignet is an employee of Merck Healthcare KGaA, Darmstadt, Germany.

Open Access This article is licensed under a Creative Commons Attribution 4.0 International License, which permits use, sharing, adaptation, distribution and reproduction in any medium or format, as long as you give appropriate credit to the original author(s) and the source, provide a link to the Creative Commons licence, and indicate if changes were made. The images or other third party material in this article are included in the article's Creative Commons licence, unless indicated otherwise in a credit line to the material. If material is not included in the article's Creative Commons licence and your intended use is not permitted by statutory regulation or exceeds the permitted use, you will need to obtain permission directly from the copyright holder. To view a copy of this licence, visit <http://creativecommons.org/licenses/by/4.0/>.

References

- Lieu CH, Tan A-C, Leong S, Diamond JR, Eckhardt SG (2013) From bench to bedside: lessons learned in translating preclinical studies in cancer drug development. *JNCI J Natl Cancer Inst* 105:1441–1456. <https://doi.org/10.1093/jnci/djt209>
- Seyhan AA (2019) Lost in translation: the valley of death across preclinical and clinical divide—identification of problems and overcoming obstacles. *Transl Med Commun* 4:18. <https://doi.org/10.1186/s41231-019-0050-7>
- Langdon SP, Hendriks HR, Braakhuis B-JM, Pratesi G, Berger DP, Fodstad Ø et al (1994) Preclinical phase II studies in human tumor xenografts: a European multicenter follow-up study. *Ann Oncol* 5:415–422. <https://doi.org/10.1093/oxfordjournals.annonc.a058872>
- Kerbel RS, Guerin E, Francia G, Xu P, Lee CR, Ebos JML et al (2013) Preclinical recapitulation of antiangiogenic drug clinical efficacies using models of early or late stage breast cancer metastasis. *Breast* 22:S57–65. <https://doi.org/10.1016/j.breast.2013.07.011>
- Kola I, Landis J (2004) Can the pharmaceutical industry reduce attrition rates? *Nat Rev Drug Discov* 3:711–715. <https://doi.org/10.1038/nrd1470>
- Wong H, Choo EF, Alicke B, Ding X, La H, McNamara E et al (2012) Antitumor activity of targeted and cytotoxic agents in murine subcutaneous tumor models correlates with clinical response. *Clin Cancer Res* 18:3846–3855. <https://doi.org/10.1158/1078-0432.CCR-12-0738>
- Gao H, Korn JM, Ferretti S, Monahan JE, Wang Y, Singh M et al (2015) High-throughput screening using patient-derived tumor xenografts to predict clinical trial drug response. *Nat Med* 21:1318–1325. <https://doi.org/10.1038/nm.3954>
- Owonikoko TK, Zhang G, Kim HS, Stinson RM, Bechara R, Zhang C et al (2016) Patient-derived xenografts faithfully replicated clinical outcome in a phase II co-clinical trial of arsenic trioxide in relapsed small cell lung cancer. *J Transl Med* 14:111. <https://doi.org/10.1186/s12967-016-0861-5>
- Ireson CR, Alavijeh MS, Palmer AM, Fowler ER, Jones HJ (2019) The role of mouse tumour models in the discovery and development of anticancer drugs. *Br J Cancer* 121:101–108. <https://doi.org/10.1038/s41416-019-0495-5>
- Devita VT, Young RC, Canellos GP (1975) Combination versus single agent chemotherapy: a review of the basis for selection of drug treatment of cancer. *Cancer* 35:98–110. [https://doi.org/10.1002/1097-0142\(197501\)35:1%3c98::AID-CNCR2820350115%3e3.0.CO;2-B](https://doi.org/10.1002/1097-0142(197501)35:1%3c98::AID-CNCR2820350115%3e3.0.CO;2-B)
- Komarova NL, Boland CR (2013) Calculated treatment. *Nature* 499:291–292. <https://doi.org/10.1038/499291a>
- Al-Lazikani B, Banerji U, Workman P (2012) Combinatorial drug therapy for cancer in the post-genomic era. *Nat Biotechnol* 30:679–692. <https://doi.org/10.1038/nbt.2284>
- Mould D, Walz A-C, Lave T, Gibbs J, Frame B (2015) Developing exposure/response models for anticancer drug treatment: special considerations. *CPT Pharmacomet Syst Pharmacol* 4:e00016. <https://doi.org/10.1002/psp4.16>
- Chu X, Bleasby K, Evers R (2013) Species differences in drug transporters and implications for translating preclinical findings to humans. *Expert Opin Drug Metab Toxicol* 9:237–252. <https://doi.org/10.1517/17425255.2013.741589>
- Vakil V, Trappe W (2019) Drug combinations: mathematical modeling and networking methods. *Pharmaceutics* 11:208. <https://doi.org/10.3390/pharmaceutics11050208>
- Simeoni M, Magni P, Cammia C, Nicolao GD, Croci V, Pesenti E et al (2004) Predictive pharmacokinetic-pharmacodynamic modeling of tumor growth kinetics in xenograft models after

- administration of anticancer agents. *Cancer Res* 64:1094–1101. <https://doi.org/10.1158/0008-5472.CAN-03-2524>
17. Gabrielson J, Gibbons FD, Peletier LA (2016) Mixture dynamics: combination therapy in oncology. *Eur J Pharm Sci* 88:132–146. <https://doi.org/10.1016/j.ejps.2016.02.020>
18. Cardilin T, Almquist J, Jirstrand M, Sostelly A, Amendt C, El Bawab S et al (2017) Tumor static concentration curves in combination therapy. *AAPS J* 19:456–467. <https://doi.org/10.1208/s12248-016-9991-1>
19. Stein S, Zhao R, Haeno H, Vivanco I, Michor F (2018) Mathematical modeling identifies optimum lapatinib dosing schedules for the treatment of glioblastoma patients. *PLOS Comput Biol* 14:e1005924. <https://doi.org/10.1371/journal.pcbi.1005924>
20. Zhu AZ (2018) Quantitative translational modeling to facilitate preclinical to clinical efficacy & toxicity translation in oncology. *Future Sci OA* 4:FSO306. <https://doi.org/10.4155/fsoa-2017-0152>
21. Bottino DC, Patel M, Kadakia E, Zhou J, Patel C, Neuwirth R et al (2019) Dose optimization for anticancer drug combinations: maximizing therapeutic index via clinical exposure-toxicity/preclinical exposure-efficacy modeling. *Clin Cancer Res* 25:6633–6643. <https://doi.org/10.1158/1078-0432.CCR-18-3882>
22. Lindauer A, Valiathan CR, Mehta K, Sriram V, de Greef R, Ellassaïss-Schaap J et al (2017) Translational pharmacokinetic/pharmacodynamic modeling of tumor growth inhibition supports dose-range selection of the anti-PD-1 antibody pembrolizumab. *CPT Pharmacomet Syst Pharmacol* 6:11–20. <https://doi.org/10.1002/psp4.12130>
23. Mak IW, Evaniew N, Ghert M (2014) Lost in translation: animal models and clinical trials in cancer treatment. *Am J Transl Res* 6:114–118
24. Spilker ME, Chen X, Visswanathan R, Vage C, Yamazaki S, Li G et al (2017) Found in translation: maximizing the clinical relevance of nonclinical oncology studies. *Clin Cancer Res* 23:1080–1090. <https://doi.org/10.1158/1078-0432.CCR-16-1164>
25. Luo FR, Yang Z, Dong H, Camuso A, McGlinchey K, Fager K et al (2005) Prediction of active drug plasma concentrations achieved in cancer patients by pharmacodynamic biomarkers identified from the geo human colon carcinoma xenograft model. *Clin Cancer Res* 11:5558–5565. <https://doi.org/10.1158/1078-0432.CCR-05-0368>
26. Center for Drug Evaluation and Research. Multi-Disciplinary Review and Evaluation NDA 210498 MEKTOVI™ 2015.
27. Mansoori B, Mohammadi A, Davudian S, Shirjang S, Baradaran B (2017) The different mechanisms of cancer drug resistance: a brief review. *Adv Pharm Bull* 7:339–348. <https://doi.org/10.15171/apb.2017.041>
28. Eisenhauer EA, Therasse P, Bogaerts J, Schwartz LH, Sargent D, Ford R et al (2009) New response evaluation criteria in solid tumours: revised RECIST guideline (version 1.1). *Eur J Cancer* 45:228–247. <https://doi.org/10.1016/j.ejca.2008.10.026>
29. Dummer R, Schadendorf D, Ascierto PA, Arance A, Dutriaux C, Giacomo AMD et al (2017) Binimetinib versus dacarbazine in patients with advanced NRAS-mutant melanoma (NEMO): a multicentre, open-label, randomised, phase 3 trial. *Lancet Oncol* 18:435–445. [https://doi.org/10.1016/S1470-2045\(17\)30180-8](https://doi.org/10.1016/S1470-2045(17)30180-8)
30. Ascierto PA, Schadendorf D, Berking C, Agarwala SS, van Herpen CM, Queirolo P et al (2013) MEK162 for patients with advanced melanoma harbouring NRAS or Val600 BRAF mutations: a non-randomised, open-label phase 2 study. *Lancet Oncol* 14:249–256. [https://doi.org/10.1016/S1470-2045\(13\)70024-X](https://doi.org/10.1016/S1470-2045(13)70024-X)
31. Sosman JA, Kittaneh M, Lolkema MPJK, Postow MA, Schwartz G, Franklin C et al (2014) A phase 1b/2 study of LEE011 in combination with binimetinib (MEK162) in patients with NRAS-mutant melanoma: early encouraging clinical activity. *J Clin Oncol* 32:9009–9009. https://doi.org/10.1200/jco.2014.32.15_suppl.9009
32. Dummer R, Ascierto PA, Gogas HJ, Arance A, Mandalá M, Liszkay G et al (2018) Encorafenib plus binimetinib versus vemurafenib or encorafenib in patients with BRAF-mutant melanoma (COLUMBUS): a multicentre, open-label, randomised phase 3 trial. *Lancet Oncol* 19:603–615. [https://doi.org/10.1016/S1470-2045\(18\)30142-6](https://doi.org/10.1016/S1470-2045(18)30142-6)
33. Cunningham D, Humblet Y, Siena S, Khayat D, Bleiberg H, Santoro A et al (2004) Cetuximab monotherapy and cetuximab plus irinotecan in irinotecan-refractory metastatic colorectal cancer. *N Engl J Med* 351:337–345. <https://doi.org/10.1056/NEJMoa033025>
34. Kopetz S, Grothey A, Yaeger R, Cutsem EV, Desai J, Yoshino T et al (2019) Encorafenib, binimetinib, and cetuximab in BRAF V600E-mutated colorectal cancer. *N Engl J Med* 381:1632–1643. <https://doi.org/10.1056/NEJMoa1908075>
35. European Medicines Agency. Assessment report Braftovi Procedure No. EMEA/H/C/004580/0000 2018.
36. European Medicines Agency. Assessment report Kisqali Procedure No. EMEA/H/C/004213/0000 2017.
37. Center for Drug Evaluation and Research. Pharmacology Review of Cotellic n.d.
38. European Medicines Agency. Scientific Discussion on Erbitux 2004.
39. Hayes SA, Pietanza MC, O'Driscoll D, Zheng J, Moskowitz CS, Kris MG et al (2016) Comparison of CT volumetric measurement with RECIST response in patients with lung cancer. *Eur J Radiol* 85:524–533. <https://doi.org/10.1016/j.ejrad.2015.12.019>
40. Schiavon G, Ruggiero A, Schöffski P, van der Holt B, Bekers DJ, Eechoute K et al (2012) Tumor volume as an alternative response measurement for imatinib treated GIST patients. *PLoS One* 7:e48372. <https://doi.org/10.1371/journal.pone.0048372>
41. West GB, Woodruff WH, Brown JH (2002) Allometric scaling of metabolic rate from molecules and mitochondria to cells and mammals. *Proc Natl Acad Sci USA* 99(Suppl 1):2473–2478. <https://doi.org/10.1073/pnas.012579799>
42. Herman AB, Savage VM, West GB (2011) A quantitative theory of solid tumor growth, metabolic rate and vascularization. *PLoS One* 6:e22973. <https://doi.org/10.1371/journal.pone.0022973>
43. Leander J, Almquist J, Johnning A, Larsson J, Jirstrand M (2021) Nonlinear mixed effects modeling of deterministic and stochastic dynamical systems in wolfram mathematica. *IFAC-Pap* 54:409–414. <https://doi.org/10.1016/j.ifacol.2021.08.394>
44. Bohnert T, Gan L-S (2013) Plasma protein binding: from discovery to development. *J Pharm Sci* 102:2953–2994. <https://doi.org/10.1002/jps.23614>
45. Smith DA, Di L, Kerns EH (2010) The effect of plasma protein binding on in vivo efficacy: misconceptions in drug discovery. *Nat Rev Drug Discov* 9:929–939. <https://doi.org/10.1038/nrd3287>
46. Choo EF, Ng CM, Berry L, Belvin M, Lewin-Koh N, Merchant M et al (2013) PK-PD modeling of combination efficacy effect from administration of the MEK inhibitor GDC-0973 and PI3K inhibitor GDC-0941 in A2058 xenografts. *Cancer Chemother Pharmacol* 71:133–143. <https://doi.org/10.1007/s00280-012-1988-6>
47. Goteti K, Garner CE, Utley L, Dai J, Ashwell S, Moustakas DT et al (2010) Preclinical pharmacokinetic/pharmacodynamic models to predict synergistic effects of co-administered anti-cancer agents. *Cancer Chemother Pharmacol* 66:245–254. <https://doi.org/10.1007/s00280-009-1153-z>
48. Kaplan FM, Shao Y, Mayberry MM, Aplin AE (2011) Hyperactivation of MEK–ERK1/2 signaling and resistance to apoptosis induced by the oncogenic B-RAF inhibitor, PLX4720, in mutant N-RAS melanoma cells. *Oncogene* 30:366–371. <https://doi.org/10.1038/ncr.2010.408>
49. Jain RK, Lee JJ, Ng C, Hong D, Gong J, Naing A et al (2012) Change in tumor size by RECIST correlates linearly with overall

- survival in phase I oncology studies. *J Clin Oncol Off J Am Soc Clin Oncol* 30:2684–2690. <https://doi.org/10.1200/JCO.2011.36.4752>
50. Nishino M, Dahlberg SE, Cardarella S, Jackman DM, Rabin MS, Hatabu H et al (2013) Tumor volume decrease at 8 weeks is associated with longer survival in EGFR-mutant advanced non-small-cell lung cancer patients treated with EGFR TKI. *J Thorac Oncol Off Publ Int Assoc Study Lung Cancer* 8:1059–1068. <https://doi.org/10.1097/JTO.0b013e318294c909>
 51. Liu F, Zhao B, Krug LM, Ishill NM, Lim RC, Guo P et al (2010) Assessment of therapy responses and prediction of survival in malignant pleural mesothelioma through computer-aided volumetric measurement on computed tomography scans. *J Thorac Oncol Off Publ Int Assoc Study Lung Cancer* 5:879–884. <https://doi.org/10.1097/JTO.0b013e3181dd0ef1>
 52. Jumbe NL, Xin Y, Leipold DD, Crocker L, Dugger D, Mai E et al (2010) Modeling the efficacy of trastuzumab-DM1, an antibody drug conjugate, in mice. *J Pharmacokinet Pharmacodyn* 37:221–242. <https://doi.org/10.1007/s10928-010-9156-2>
 53. Pierrillas PB, Henin E, Ogier J, Amiel M, Kraus-Berthier L, Chenel M et al (2020) Translational approach from preclinical to clinical: comparison of dose finding methods of a new Bcl2 inhibitor using PK-PD modeling and interspecies extrapolation. *Invest New Drugs* 38:1796–1806. <https://doi.org/10.1007/s10637-020-00953-y>

Publisher's Note Springer Nature remains neutral with regard to jurisdictional claims in published maps and institutional affiliations.